VIP Interfaces

DOI: 10.1002/anie.201000108

Janus Microspheres for a Highly Flexible and Impregnable Water-Repelling Interface**

Shin-Hyun Kim, Su Yeon Lee, and Seung-Man Yang**

As part of the evolutionary drive to survive and reproduce, some organisms have developed unique surface morphologies. For example, mosquitoes have anti-fog compound eyes that are decorated with small boss arrays,[1] and some desert beetles have patterned wings that enable them to collect water droplets from the atmosphere.[2] Geckos can climb vertical walls and even hang upside down from the ceiling because of spatula arrays on their footpads.[3,4] Many researchers have sought to mimic such natural surface morphologies to develop useful materials. Artificial superhydrophobic surfaces, which are a representative group of biomimetic materials, have great potential in a wide range of industrial applications owing to their self-cleaning, anti-fogging, and anti-biofouling properties.[5–8] Natural water-repelling objects, such as sundews and lotus leaves, butterfly wings, and duck feathers, have inspired researchers to explore various morphologies, ranging from disordered[9–13] to highly textured surfaces,[14–19] in efforts to prepare superhydrophobic surfaces on solid films. However, most studies on superhydrophobic materials performed to date have focused on methods for preparing flat solid surfaces in an inexpensive and simple manner.[8]

Herein, we have sought to develop superhydrophobic materials that do not require flat substrates. Taking inspiration from superhydrophobic small objects, such as the scales of butterflies or moths and the legs of water striders,[20,21] we fabricated and investigated superhydrophobic microspheres with a complex surface morphology in conjunction with hydrophobic surface moieties. The high mobility of the superhydrophobic microspheres gives rise to unique interfacial properties that cannot be achieved using conventional superhydrophobic materials of solid film type.

To create the complex surface morphology on the microspheres, we employed emulsion droplets (a Pickering emulsion) decorated with silica particles as a template.[22] Droplets of the photocurable resin ethoxylated trimethylolpropane triacrylate (ETPTA) containing silica particles were generated, and microspheres with silica particle arrays on their surfaces were obtained after photopolymerization of the droplet phase. Through subsequent selective removal of the silica particles by a wet-etching process, we obtained microspheres with surfaces covered with cavity arrays. Further to creating the complex morphology, we incorporated a hydrophobic moiety on the surface to achieve superhydrophobicity, which was achieved simply by applying reactive ion etching (RIE) with sulfur hexafluoride. These procedures are summarized in Figure 1 a.

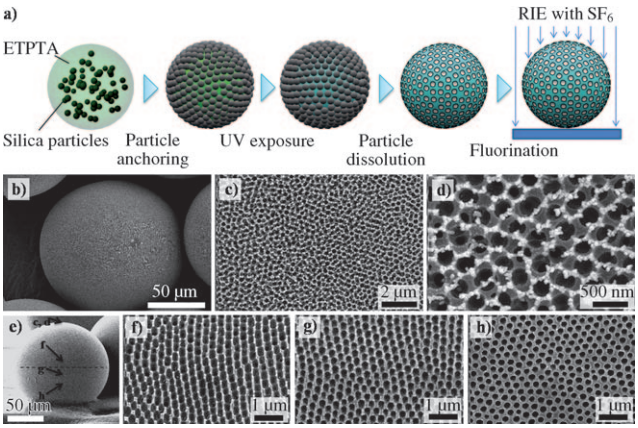

Figure 1. a) Preparation of Janus microspheres with superhydrophobic and hydrophilic faces. b–d) SEM images of the top surface of a RIE-treated microsphere at three different magnifications. e) Side view of microspheres bonded on a flat substrate with adhesive tape. f–h) Surface morphologies of microspheres at the positions denoted in (e).

Highly monodisperse emulsion droplets were generated in dripping mode using co-flowing streams of ETPTA suspension and aqueous surfactant solution in a glass capillary device composed of two coaxial capillaries.[23] Highly monodisperse emulsion droplets of ETPTA-containing silica particles (10 % wt/wt) and iron oxide nanoparticles (0.2 % wt/wt) were generated at the constant rate of 60 droplets per second (Supporting Information, Figure S1 and Movie S1). After droplet generation, the emulsion was left to stand for 10 min to allow migration of the silica particles to the free interface and protrusion into the continuous phase whilst the nanoparticles remained inside the droplets owing to their hydrophobic nature. The anchoring of silica particles at the droplet interface reduces the total interfacial energy, which is contributed from three interfaces between silica–ETPTA, silica–water and ETPTA–water.[22] Next, the droplets were

[*] Dr. S.-H. Kim, S. Y. Lee, Prof. S.-M. Yang
National Creative Research Initiative Center for
Integrated Optofluidic Systems and
Department of Chemical and Biomolecular Engineering, KAIST
Daejeon, 305-701 (Korea)
Fax: (+82) 42-350-5962
E-mail: dmz@kaist.ac.kr
smyang@kaist.ac.kr
Homepage: http://msfl.kaist.ac.kr

[**] This work was supported by a grant from the Creative Research Initiative Program of the Ministry of Education, Science, and Technology for "Complementary Hybridization of Optical and Fluidic Devices for Integrated Optofluidic Systems".

Supporting information for this article is available on the WWW under http://dx.doi.org/10.1002/anie.201000108.

photopolymerized by applying UV irradiation for 2 seconds. This process resulted in microspheres decorated with a hexagonal array of silica particles. The average contact angle of the silica-decorated microspheres at the air–water interface was 10°, which is smaller than the angle of 37° observed for microspheres with a smooth surface owing to the hydrophilic silica particle arrays (Supporting Information, Figure S2 a–d). After removal of the silica particles by wet etching, the microspheres exhibited two distinctive contact angles depending on whether the cavities on their surfaces were filled with water or air. When the cavities were occupied with water, the average contact angle was 29°. In contrast, the average contact angle for microspheres with cavities occupied with air was 72°. These values for water- and air-filled cavities roughly coincide with the values of 30° and 80°, respectively, obtained using the Cassie–Baxter relation,[5,6] for which the relative fractions of ETPTA and cavities were calculated from an SEM image (Supporting Information, Figure S2 e–g).

To modify the surface properties of the microspheres, we applied RIE with SF_6. To achieve this, a monolayer of microspheres with cavity arrays was deposited on polydimethylsiloxane (PDMS) film, and a directional flow of reactive ions of SF_6 was then applied; during this process, the strong adhesion of the microspheres to the PDMS substrate prevented their movement (Supporting Information, Figure S3). The RIE dramatically altered the surface properties through both fluorination and creation of a complex highly porous surface. Figure 1 b shows a RIE-treated microsphere with a moiré fringe. At higher magnifications (Figure 1 c,d), we can observe the hexagonal arrangement of cavities and enhanced porosity with larger and deeper surface cavities in comparison with the microspheres before RIE (Supporting Information, Figure S2e). To determine whether RIE induces fluorination of ETPTA surfaces, we applied RIE to a smooth ETPTA film and examined the RIE-induced change in water contact angle and X-ray photoelectron spectroscopy (XPS) data. The RIE treatment increased the contact angle of a water droplet on the film from 43° to 100° and caused the emergence of a strong XPS peak associated with fluorine at 685 eV (Supporting Information, Figure S4).

In the RIE process applied to the microsphere monolayer, the directionality of the reactive ion flow induces anisotropic etching and thus gives rise to distinct surface morphologies depending on the location on the microsphere surface with respect to the reactive ion flow (Figure 1 e). Unlike the top surface of each sphere (Figure 1 c,d), the side surface slightly above the equator exhibits vertically aligned needle arrays (Figure 1 f). On the other hand, the surface immediately below the equator is less affected (Figure 1 g), and the original surface morphology remains intact in the region of the sphere near the substrate (Figure 1 h). Therefore, each microsphere can have a superhydrophobic top hemisphere combined with a hydrophilic bottom hemisphere (contact angle ca. 72°).

We then prepared a monolayer of these Janus microspheres at the air–water interface.[24,25] As expected, the superhydrophobic and hydrophilic surfaces of the microspheres faced the air and water phases, respectively. The monodisperse microspheres formed a hexagonal array at the interface (Supporting Information, Figure S5); the contact line was invisible because the contact angle exceeded 90°. The microspheres appear brown in color owing to the incorporation of iron oxide nanoparticles into the microspheres. Upon dropping water onto the monolayer of Janus microspheres at the water–air interface (Figure 2 a,b; Supporting Information, Movie S2), the water formed a spherical droplet 2.4 mm in diameter on the surface that is comprised of superhydrophobic hemispheres. Because the hydrophilic surfaces of the microspheres were strongly held by the water phase, the microspheres did not attach to the surface of the added water droplet. Figure 2 c–f shows optical microscope images of the monolayer of microspheres and an added droplet of diameter 0.85 mm, respectively; the images in Figure 2 d–f were taken at three different focal planes. When however we employed ETPTA microspheres with smooth surfaces that were treated with the same RIE procedure, droplets placed on the microsphere-anchored interface immediately burst through into the water phase, regardless of the droplet size. (For comparison, the behavior of water droplets on superhydrophobic and smooth Janus microsphere monolayers and magnetic manipulation of the superhydrophobic microspheres at the air–water interface can be seen in the Supporting Information, Movie S2.)

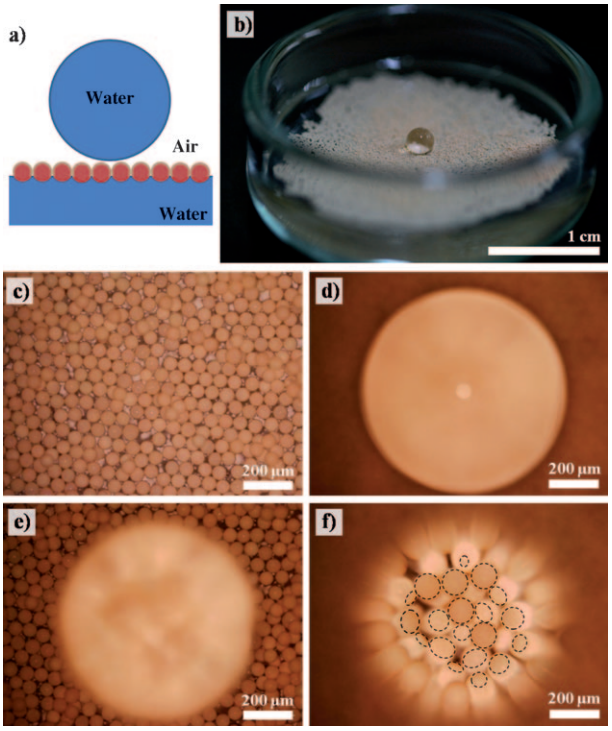

Figure 2. a,b) Model (a) and optical image (b) of a water droplet sitting on an air–water interface protected by a monolayer of Janus microspheres. c) Optical microscope (OM) image of an array of Janus microspheres anchored at an air–water interface. d–f) OM images of a water droplet taken at three different focal planes parallel to the equator of the droplet (d), microsphere array surface in the vicinity of the droplet (e), and microsphere array surface below the droplet (f). The dashed circles in (f) denote the contact line of the water droplet on a microsphere.

When droplets larger than 2.5 mm in diameter were placed on an incompletely filled monolayer at the air–water interface, the gravitational force on the droplet was sufficient to cause most such droplets to fall into the water bath within a few seconds by widening the interstices between the microspheres. However, when a completely filled interface was used, the microspheres at the interface created a highly flexible superhydrophobic barrier. For example, a completely filled microsphere layer prevented direct contact between a hydrophilic glass stick and the underlying water phase (Figure 3a,b). It can be clearly seen that the glass stick is

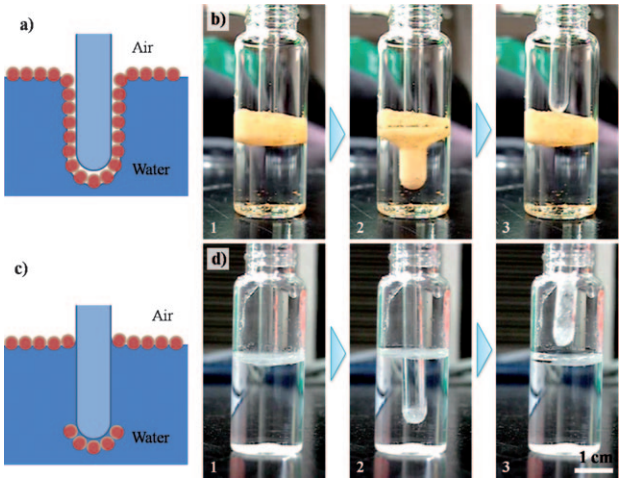

Figure 3. a) The response of a Janus microsphere monolayer to intrusion by a hydrophilic stick, thus demonstrating how the monolayer acts as a flexible barrier at the air–water interface. b) Sequential images of an air–water interface protected with a monolayer of Janus microspheres with porous surfaces. c) Failure of a Janus microsphere monolayer when subjected to poking by an external stick. d) Images showing the breakdown of a protective layer composed of Janus microspheres with smooth surfaces.

completely enclosed with aligned microspheres at the interface, and that no microspheres remain on the surface of the stick after removal. However, when the same experiment was performed using RIE-treated smooth microspheres, the glass stick immediately penetrated the microsphere layer and entered the underlying water phase, and numerous microspheres remained coated on the surface of the stick after its removal (Figure 3c,d). (The dynamic motion of a highly flexible barrier comprised of superhydrophobic Janus microspheres and the failure of the smooth microsphere layer shown in the Supporting Information, Movie S3.)

The Janus microspheres with both superhydrophobic and hydrophilic surfaces can be used to make liquid marbles: each marble is comprised of a water droplet completely covered with Janus microspheres and their hydrophilic surfaces are directed toward the center of the droplet.[26,27] By rolling a water droplet on a pile of microspheres, a microsphere-decorated spherical droplet could be created (Figure 4a,b). The optical microscope images of the liquid marble (Figure 4c,d) show the hexagonal arrangement of the microspheres at the interface, which form a contact angle of approximately 120°. Such liquid marbles could be handled

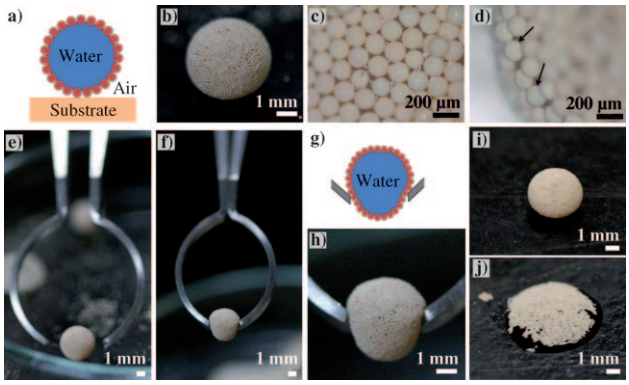

Figure 4. a,b) Model (a) and optical image (b) of a liquid marble composed of a water droplet coated with Janus microspheres. c,d) OM images showing the surface of a liquid marble in the top (c) and edge (d) regions. The arrows denote the contact line of the microspheres at the air–water interface. e–h) Images showing a liquid marble being picked up with a pair of tweezers. The spherical liquid marble shown in (e) deformed after pressing with the tweezers. i) Liquid marble after being released from the tweezers in a height of 1 cm. j) Failure of a liquid marble that was dropped onto a substrate from a height of 10 cm.

with tweezers (Figure 4e–h). Because the close-packed monolayer of microspheres at the interface can support unequal stresses, liquid marbles (that is, interfacial composite materials) can have mechanical properties quite different from those of simple water droplets and solid materials.[28] For example, when a marble was picked up with tweezers, it deformed owing to the applied mechanical force, and it maintained the deformed shape when held by the tweezers (Figure 4h). When liquid marbles whose surfaces were not completely covered with microspheres were picked up with tweezers, they sometimes slipped off the tweezers by deforming their shape without bursting of the water drop. Upon dropping a liquid marble onto a table from a height of 1 cm, the liquid marble took on an oblate spheroid shape (Figure 4i). However, marbles dropped from a height of 10 cm height burst on the table surface (Figure 4j). In the latter case, the high inertia of the water drop induces deformation of the interface shape in the interstices between the microspheres, leading to contact between the water and the table surface. (The preparation of a liquid marble, blowing or magnet-induced control of the motion of a marble, and picking up a liquid marble with a pair of tweezers are shown in the Supporting Information, Movie S4, and drying behavior of liquid marbles is described in Figure S6.)

In conclusion, we have prepared Janus microspheres composed of superhydrophobic and hydrophilic surfaces by a process that commences with photocurable Pickering emulsion droplets. When the Janus microspheres were placed at an air–water interface, they acted as a highly flexible superhydrophobic barrier in which the hydrophilic surfaces were strongly held and aligned along the interface. The membrane of Janus microspheres remained stable when a water droplet was placed on it, and even maintained its integrity under a dynamic disturbance induced by a hydrophilic glass stick. Furthermore, the Janus microspheres could be used to prepare liquid marbles that could be manipulated with

magnets or tweezers. We believe that superhydrophobic small objects have great potential in size-dependent semipermeable membranes along interfaces between immiscible fluids, buoys for water floating micromachines, and various superhydrophobic coatings, especially in the context of rain- and tear-resistant makeup.

Experimental Section

Silica particles 245 nm in diameter were prepared by sol–gel chemistry using the Stöber method. An ethanolic suspension of the silica particles and iron oxide (α-Fe_2O_3) nanoparticles (< 50 nm, Aldrich) was mixed with ETPTA resin (Aldrich) containing a photoinitiator (Irgacure2100, Ciba Specialty Chemicals). After mixing was complete, the ethanol was selectively evaporated for 12 h at 70 °C; the quantities of silica particles and α-Fe_2O_3 nanoparticles were chosen such that their weight fractions in the final ethanol-free ETPTA suspension would be 10% and 0.2% (wt/wt), respectively. The suspension was sonicated for 30 min prior to its use for droplet generation.

Monodisperse droplets were generated using a microfluidic device composed of two coaxial capillaries. For stable droplet generation in the dripping regime, the flow rate of the dispersed phase (photocurable suspension) was kept low relative to that of the continuous phase (aqueous surfactant solution of 1 wt.% ethylene oxide–propylene oxide–ethylene oxide triblock copolymer, Pluronic F108; BASF). Ten minutes after droplet generation, the prepared monodisperse droplets were photopolymerized by UV irradiation for 2 seconds.

To create a complex surface morphology, we treated the microspheres with 5% HF (Sigma–Aldrich) for 5 min. The resulting microspheres with porous surfaces were washed several times with water and dried. To provide fluorine groups and higher porosity on the microsphere surfaces, RIE (VSRIE-400A, Vacuum Science) with 100 sccm SF_6 was applied to a monolayer of microspheres on a PDMS film for 30 seconds at 150 W.

Received: January 8, 2010
Published online: March 15, 2010

Keywords: colloids · Janus particles · Pickering emulsions · superhydrophobicity

[1] X. Gao, X. Yan, X. Yao, L. Xu, K. Zhang, J. Zhang, B. Yang, L. Jiang, *Adv. Mater.* **2007**, *19*, 2213.
[2] L. Zhai, M. C. Berg, F. C. Cebeci, Y. Kim, J. M. Milwid, M. F. Rubner, R. E. Cohen, *Nano Lett.* **2006**, *6*, 1213.
[3] K. Autumn, Y. A. Liang, S. T. Hsieh, W. Zesch, W. P. Chan, T. W. Kenny, R. Fearing, R. J. Full, *Nature* **2000**, *405*, 681.
[4] H. Lee, B. P. Lee, P. B. Messersmith, *Nature* **2007**, *448*, 338.
[5] A. Lafuma, D. Quere, *Nat. Mater.* **2003**, *2*, 457.
[6] P. de Gennes, F. Brochard-Wyart, D. Quere, *Capillarity and Wetting Phenomena: Drops, Bubbles, Pearls, Waves*, Springer, Paris, **2004**, chap. 9.
[7] R. Blossey, *Nat. Mater.* **2003**, *2*, 301.
[8] P. Roach, N. J. Shirtcliffe, M. I. Newton, *Soft Matter* **2008**, *4*, 224.
[9] S. Shibuichi, T. Onda, N. Satoh, K. Tsujii, *J. Phys. Chem.* **1996**, *100*, 19512.
[10] K. K. S. Lau, J. Bico, K. B. K. Teo, M. Chhowalla, G. A. J. Amaratunga, W. I. Milne, G. H. Mckinley, K. K. Gleason, *Nano Lett.* **2003**, *3*, 1701.
[11] L. Jiang, Y. Zhao, J. Zhai, *Angew. Chem.* **2004**, *116*, 4438; *Angew. Chem. Int. Ed.* **2004**, *43*, 4338.
[12] J.-M. Lim, G.-R. Yi, J. H. Moon, C.-J. Heo, S.-M. Yang, *Langmuir* **2007**, *23*, 7981.
[13] W. Song, D. D. Veiga, C. A. Custodio, J. F. Mano, *Adv. Mater.* **2009**, *21*, 1830.
[14] D. Öner, T. J. McCarthy, *Langmuir* **2000**, *16*, 7777.
[15] J.-Y. Shiu, C.-W. Kuo, P. Chen, C.-Y. Mou, *Chem. Mater.* **2004**, *16*, 561.
[16] T. N. Krupenkin, J. A. Taylor, T. M. Schneider, S. Yang, *Langmuir* **2004**, *20*, 3824.
[17] H. Yabu, M. Takebayashi, M. Tanaka, M. Shimomura, *Langmuir* **2005**, *21*, 3235.
[18] Y. Kwon, N. Patankar, J. Choi, J. Lee, *Langmuir* **2009**, *25*, 6129.
[19] A. Tuteja, W. Choi, M. Ma, J. M. Mabry, S. A. Mazzella, G. C. Rutledge, G. H. Mckinley, R. E. Cohen, *Science* **2007**, *318*, 1618.
[20] Y. Zheng, X. Gao, K. Jiang, *Soft Matter* **2007**, *3*, 178.
[21] X. Gao, L. Jiang, *Nature* **2004**, *432*, 36.
[22] B. P. Binks, S. O. Lumsdon, *Langmuir* **2000**, *16*, 8622.
[23] A. S. Utada, A. Fernandez-Nieves, H. A. Stone, D. A. Weitz, *Phys. Rev. Lett.* **2007**, *99*, 094502.
[24] J.-W. Kim, D. Lee, H. C. Shum, D. A. Weitz, *Adv. Mater.* **2008**, *20*, 3239.
[25] N. Glaser, D. J. Adams, A. Boker, G. Krausch, *Langmuir* **2006**, *22*, 5227.
[26] P. Aussillous, D. Quere, *Nature* **2001**, *411*, 924.
[27] D. Dupin, S. P. Armes, S. Fujii, *J. Am. Chem. Soc.* **2009**, *131*, 5386.
[28] A. Bala Subramaniam, M. Abkarian, H. A. Stone, *Nature* **2005**, *438*, 930.

